Time-Domain Adaptive Feed-Forward Control of Nanopositioning Systems with Periodic Inputs

Andrew J. Fleming

Abstract— This paper describes a method for feedforward tracking control of linear and non-linear systems with periodic desired trajectories. The method utilizes adaptive Finite Impulse Response (FIR) filters to realize an adaptive inverse control scheme. Compared to previously reported frequency domain methods, this technique can be implemented in real-time and generates a coefficient update every sampling instance.

The proposed method is successfully applied to the adaptive inverse control of an experimental nanopositioning system. The maximum RMS error during both large-range and high-speed scans was 0.23%. This is comparable to previously reported frequency-domain techniques and is far superior to the performance achievable with standard feedback methods.

I. INTRODUCTION

Mechanical scanners with periodic trajectories are found in many types of scientific and industrial machine. Such devices include beam scanners [1], manufacturing robots, cam motion generators, and scanning probe microscopes (SPMs) [2]. Of these applications, the SPM scanner has received the most attention in recent years [3], [4], [5]. This is because the positioning performance, or lack thereof, defines the microscope's imaging speed and resolution, two valuable commodities.

Although piezoelectric nanopositioning systems are designed to provide the greatest possible positioning accuracy, in practice they exhibit a number of non-ideal characteristics that severely degrade performance. These include creep, hysteresis and mechanical resonance [5]. As a result of these problems, practical nanopositioning systems require position sensors and a control system to provide satisfactory performance.

A. Feedback control

The most popular technique for control of commercial nanopositioning systems is sensor-based feedback using integral or proportional-integral control. Such controllers are simple, robust to modeling error, and due to high loop-gain at low-frequencies, effectively reduce piezoelectric non-linearity. However, the bandwidth of such controllers is severely limited by the presence of resonant mechanical modes. Techniques aimed at improving the closed-loop bandwidth are based either on inversion of resonant dynamics using a notch filter [6] or damping of resonant dynamics

[7], [8]. Although these techniques do improve closed-loop bandwidth, they also increase the amount of sensor-induced positioning noise which decreases resolution [7]. Even with the increases in closed-loop bandwidth that can be obtained, the performance is still not sufficient in many applications. For example, due to the tracking lag and sensor noise associated with closed-loop control, high-speed scanning probe microscopes currently use open-loop nanopositioners [9], [10], [11], [12].

B. Feedforward / inversion control

Feedforward or inversion based control is commonly applied to both open- and closed-loop nanopositioning systems that require improved performance [5], [13]. Good reference tracking can be achieved if the plant model or its frequency response are known with high accuracy. In addition to improved performance, other attractive characteristics of inversion based control are the lack of additive sensor noise and ease of implementation, particularly in high-speed applications [14].

The foremost difficulty with inversion based control is the lack of robustness to variations in plant dynamics, especially if the system is resonant [15], [13]. However, this problem only exists with static feedforward controllers. More recently, iterative techniques have been reported that eliminate both vibration and non-linearity in systems with periodic inputs [16]. Although such techniques originally required a reference model [16], in 2008, both *Kim and Zou* [17] and *Li and Bechhoefer* [18] presented techniques that operate without any prior system knowledge. Both techniques achieve essentially perfect tracking regardless of non-linearity or dynamics. This is an extremely desirable characteristic and was previously unobtainable prior to the publication of this work.

The only apparent disadvantage associated with iterative feedforward techniques [17], [18] is the computational complexity. As both methods operate in the frequency domain, a single iteration requires a number of input and output periods and the computation of Fourier and inverse Fourier transforms. Even considering the signal processing capabilities available in modern scanning probe microscopes, the required computations are significant.

Contribution of this work

In this work, a new time-domain feedforward controller is reported that achieves a similar level of tracking performance to frequency domain techniques [17], [18], but without the computational load. Due to the lesser computational load,

(a) P-734 Nanopositioner
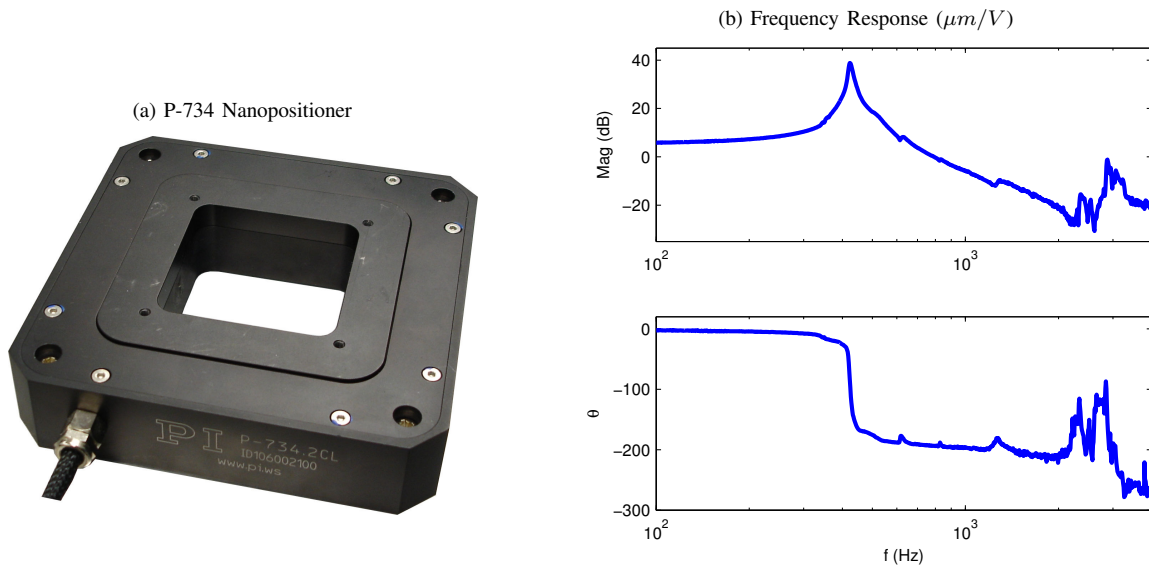
Fig. 1.   The P-734 nanopositioning platform (a), and frequency response of one axis (b) (with an amplifier gain of 20)

the proposed technique is straight-forward to implement in real-time and at high-speed. In addition, the filter coefficients are updated every sample rather than every period.

This paper continues in the next Section with a description of the experimental apparatus. This is followed by Section III that demonstrates the capability of an FIR filter to perfectly invert non-linearity and dynamics. The standard adaptive FIR filter is then reviewed in Section IV. This adaptive filter is then utilized in an adaptive inverse scheme in Section V. The paper is concluded in Section VI.

II. EXPERIMENTAL SETUP

All of the concepts discussed throughout this paper will be demonstrated on a piezoelectric nanopositioning system. Such a system is an ideal demonstration platform as it exhibits both non-linearity and a lightly-damped resonance, two challenging characteristics to control [5].

Two-axis micro- and nano-positioning stages are used extensively in many forms of scanning probe microscope. They typically comprise a pair of piezoelectric actuators, mechanical displacement amplifiers and a flexure guided sample platform. Although these configurations can achieve high precision with millimeter range motion, the internal displacement amplifiers, large piezoelectric stacks and platform mass contribute to a low mechanical resonance frequency. An example of such a stage is the Physik Intrumente P-734 pictured in Figure 1(a). This stage has a range of 100 microns but a resonance frequency of only 420 Hz. The frequency response of one axis is plotted in Figure 1(b). The position is measured with a two-plate capacitive sensor fitted to both axes, the accompanying electronics provides a full scale output of 6.7 V at 100 μm displacement.

In open-loop or with integral control, the P-734 is limited by mechanical resonance to scan frequencies of 5 Hz or less. The aim of this paper is to invert these dynamics to allow scanning at any frequency or amplitude. The only remaining
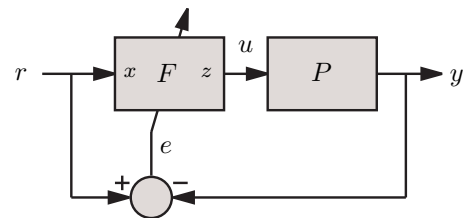
Fig. 2.   An adaptive feedforward control scheme where the input r is filtered to minimize the difference between the the desired trajectory r and plant output y

limitations should be the physical limitations imposed by the mechanics of the positioner and amplifier electronics. These limitations include the maximum tensile load of the actuators and the maximum slew-rate and current limit of the amplifier [19].

The control techniques presented are implemented using Simulink, the Real Time Workshop, and a dSpace ds1103 rapid prototyping system.

III. INVERSE MODEL STRUCTURE

The goal of a feedforward controller is to ameliorate the dynamics and non-linearity of a plant P so that a reference command r is perfectly reproduced at the plant output y. A diagram representing a feedforward control scheme is shown in Figure 2. In this diagram, the controller F is not static but its parameters are free to vary with time. The tracking error e is also available to the controller so that the parameters may be adjusted in a way that minimizes tracking error. Such a scheme is known as adaptive inverse control [20].

The starting point of any feedforward control scheme is to select a model structure for F that has sufficient complexity to represent the inverse P^{-1}. For linear systems, this choice can be straight-forward as F requires only equal or greater order than P^{-1}. However, if the system contains some form

(a) A triangular signal r being distorted by the plant P

(b) The Fourier coefficients of r in more detail
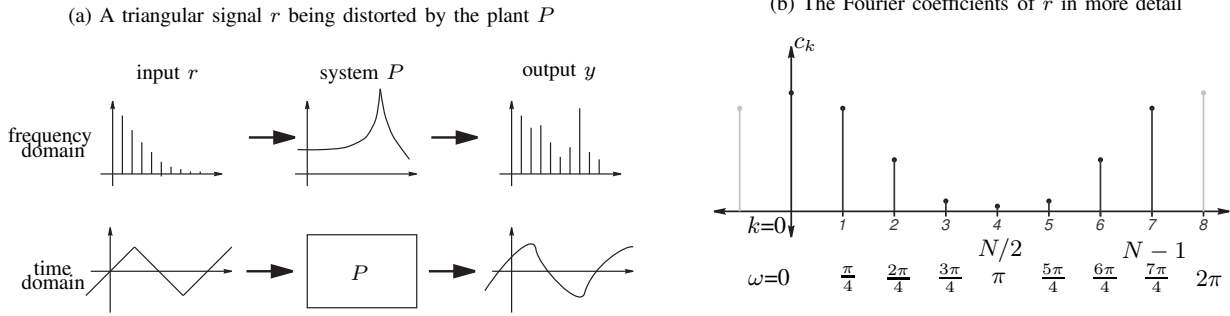
Fig. 3.   The frequency and time domain representation of a triangular scanning signal r being distorted by the dynamics and non-linearity of the plant P.

of non-linearity, the choice of inverse model immediately becomes more difficult. For piezoelectric nanopositioning systems, where the foremost non-linearity is hysteresis, model structures have included the inverse Preisach operator [21], homogenized energy models [22], polynomial methods [23] and many others [5]. Although good tracking performance has been reported, such techniques are not generally known to be accurate over a wide range of amplitudes, waveforms and frequencies.

The foremost disadvantage of a structured inverse model is its limitation to a specific type of non-linearity. A model structure that can invert any type of non-linearity is more desirable. Although this objective is in general, not possible, the problem is simplified if the reference command is periodic. If the output is also periodic and band-limited with the same fundamental frequency as the reference, the complexity of P and P^{-1} is bounded. It is this assumption of periodicity that allows a simple model structure to be used in the following.

The choice of model structure is best motivated with a frequency domain argument. Consider the triangular reference waveform r and plant output y plotted in Figure 3. The samples of r are denoted r_n where $n \in \{0, 1, 2, \cdots, N-1\}$ and N is the number of samples per period. In the illustration, the sampling frequency F_s is equal to eight times the fundamental frequency of r. Also plotted in Figure 3 is the spectrum of r and y. As the signals are periodic, the spectrum's of r and y are both line spectra defined at N frequencies between 0 and F_s, known as the harmonics [24]. Again due to periodicity, the spectral components or r and y are defined by the discrete Fourier series R_k and Y_k [24], where the analysis function is

$$R_k = \frac{1}{N} \sum_{n=0}^{N-1} r_n \, e^{-jn\frac{2\pi k}{N}}. \tag{1}$$

The synthesis function which reproduces r from R_k is [24]

$$r_n = \sum_{k=0}^{N-1} R_k \, e^{jn\frac{2\pi k}{N}}, \tag{2}$$

Due to periodicity, A key feature of the signals r and y is that they are both completely described by N Fourier coefficients. This is a strict limit on the complexity of each signal and on the required complexity of F.

To achieve perfect inversion of P regardless of dynamics and non-linearity, F requires an arbitrary frequency response at the N harmonics of r between 0 and F_s. That is,

$$F(j\omega_k) = \frac{1}{P(j\omega_k)} \quad \text{where } \omega_k \in \frac{2\pi F_s}{N} [0, 1, \cdots N - 1] \tag{3}$$

A filter that provides this required response is a Finite Impulse Response (FIR) filter of length N. Hence, this is our choice of model structure for F. Advantageously, FIR filters are the simplest form of digital filter and are computationally undemanding to implement.

The output z_n of an FIR filter is given by

$$z_n = \sum_{i=0}^{N-1} b_i x_{n-i} \tag{4}$$

where b_i are the filter coefficients and x_n is the input. This is shown diagrammatically in Figure 4.

IV. ADAPTIVE FILTERING

After finding a model structure in the previous section that allows perfect inversion of the plant P, we now wish to find a method for updating the filter parameters b_i that minimizes the tracking error e_n depicted in Figure 2. In this section, the adaptive FIR filter is reviewed as a tool for reaching this goal.

To simplify the presentation, vector notation will be used for the delayed input signal and filter weights. Referring to Figure 4, at time n, the vectors representing the delayed
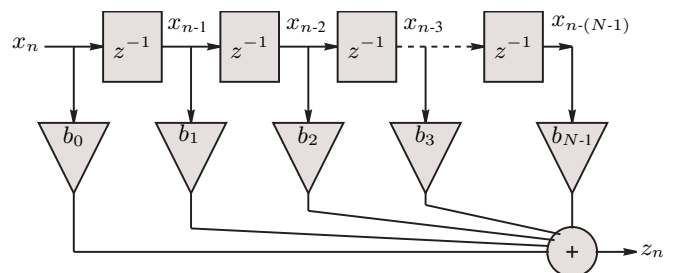
Fig. 4.   An FIR filter with input x, output z and filter coefficients **b**. This filter contains N-1 unit sample delays z^{-1}.

(a) Adaptive identification

(b) Comparison of plant and model outputs (in μm)

(c) Convergence speed - Plot of e *vs.* time (in μm)
The residual error is 0.1% RMS
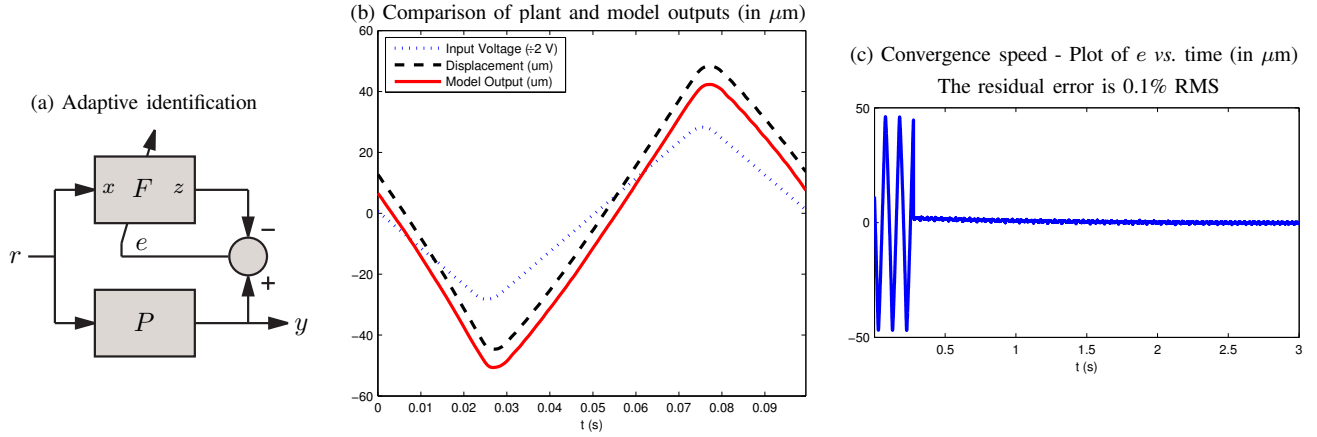
Fig. 5. Results from an adaptive system identification experiment (a) with a 10-Hz 93-μm scan. The model output in (b), which has been offset for clarity, closely matches the experimental system output with an RMS error of 0.1%. The convergence speed of the adaptive filter is shown in (c). When the adaption rate μ is switched from 0 to 1 at time t=275 mS most of the error is immediately eliminated. The small amount of residual error slowly decays after a few seconds.

samples of the input x and filter weights b_i are

$$\mathbf{x}_n = \begin{bmatrix} x_n & x_{n\text{-}1} & x_{n\text{-}2} & \cdots & x_{n\text{-}(N\text{-}1)} \end{bmatrix}^T \quad (5)$$
$$\mathbf{b}_n = \begin{bmatrix} b_0 & b_1 & b_2 & \cdots & b_{N-1} \end{bmatrix}^T .$$

With this notation the filter output is simply,

$$y_n = \mathbf{x}_n^T \mathbf{b}_n \quad (6)$$

To update the filter coefficients $\mathbf{b}$, the simplest and most commonly applied technique is the Normalized Least Mean Squares (nLMS) algorithm [25]. The new coefficients $\mathbf{b}_{n+1}$ are derived from the previous coefficients $\mathbf{b}_n$ by

$$\mathbf{b}_{n+1} = \mathbf{b}_n + 2\mu e_n \frac{\mathbf{x}_n}{\|\mathbf{x}_n\|^2}. \quad (7)$$

where μ is the update rate and $\frac{\mathbf{x}_n}{\|\mathbf{x}_n\|^2}$ is the vector $\mathbf{x}_n$, normalized by the squared 2-norm. This incredibly simple update rule is possible as the optimization associated with adaptive FIR filters is convex [25]. However, a necessary assumption is that the error e_n is equal to some desired output d_n minus the actual filter output z_n, i.e.

$$e_n = d_n - z_n. \quad (8)$$

This is a problem as it does not allow any filtering operation to occur between the filter output z and the error e, which clearly occurs in Figure 2. This precludes the direct use of adaptive FIR filters for feedforward control.

Although adaptive FIR filters cannot be directly employed in feedforward control applications, they can be utilized for tasks such as adaptive system identification. This scenario and experimental results are shown in Figure 5. In this case, the error e is directly related to the filter output z. After the error has converged to zero, the filter F has exactly the same response as the plant P. The input signal in this experiment was shaped to reduce excitation of the mechanical resonance [26]. With no oscillation, the ability of a linear filter to exactly model hysteresis is more clearly displayed. This is a unique characteristic and is only possible with periodic

inputs and the correct choice of filter length, as discussed in Section III.

V. ADAPTIVE INVERSE CONTROL

As mentioned in the previous section, adaptive FIR filters cannot be directly applied to the inverse control problem depicted in Figure 2. The reason is due to the existence of dynamics between the filter output and the error signal. These dynamics are known as secondary path dynamics [25]. To eliminate the problems experienced with secondary path dynamics, the so-called Filtered-x LMS (FXLMS) algorithm was developed [25], [20].

The FXLMS algorithm, shown pictorially in Figure 6(a), is similar to the LMS algorithm described in the previous section. The only difference is the filtering of x_n by $\hat{P}$, where $\hat{P}$ is an estimate of the plant dynamics. That is, the update rule is now

$$\mathbf{b}_{n+1} = \mathbf{b}_n + 2\mu e_n \frac{\hat{\mathbf{x}}_n}{\|\hat{\mathbf{x}}_n\|^2}. \quad (9)$$

where $\hat{\mathbf{x}}_n$ is the delayed samples of x_n filtered by $\hat{P}$.

If $\hat{P}$ closely models the actual plant dynamics, it can be proven that the beneficial properties of the LMS algorithm also extend to the FXLMS algorithm, and perfect inverse control is possible [25], [20].

The additional complexity with the FXLMS algorithm is the requirement for a plant model $\hat{P}$. As a high degree of model accuracy is not required [25], [20], many applications simply use an estimate for $\hat{P}$, obtained for example by system identification. Another approach is to actively identify $\hat{P}$ and use this model in the FXLMS algorithm. This approach is adopted here as no prior system information or identification steps are required. In the previous section, an adaptive system identification scheme was described. This scheme is directly applied in Figure 6(a) to obtain a model $\hat{P}$ of the plant. The estimated model $\hat{P}$ is then copied and also used in the FXLMS algorithm. The main drawback to

this technique is that two adaptive filters are required, one for inverse control and another for system identification.

Experimental results from adaptive inverse control of the nanopositioning system are presented in Figure 6. Two experiments are reported, one with a 10-Hz large-range reference trajectory that exhibits significant non-linearity, and another with a 76-Hz reference that exhibits a large amount of scan-induced vibration. In both cases, a control signal u was found that reduces maximum RMS error to 0.23%. This is an excellent result, far superior to what can be achieved with standard feedback methods.

In both of the experiments reported, the number of samples per period was 100. That is, the sampling frequency was 7.6 kHz during the 76 Hz scan. Using Simulink, the Real-Time Workshop, and a dSpace ds1103 DSP, the execution time required to implement the FXLMS algorithm and all data recording functions was 36 μs. This indicates a maximum sampling rate of around 27 kHz. As digital signal processors are highly optimized for the implementation of FIR filters, much faster sampling rates are possible for systems with dedicated program code and faster analog to digital converters.

VI. CONCLUSIONS

In this paper, the Filtered-x LMS algorithm (FXLMS) is applied for adaptive inverse control of a nanopositioning system. Advantageously, this technique can be implemented in real-time and generates a coefficient update every sampling instance. In experimental results, the maximum RMS error during both large-range and high-speed scanning was 0.23%. This is comparable to previously reported techniques that operate in the frequency domain.

Future work will involve investigation of different adaption rules and consideration of input signal magnitude. Although the FXLMS algorithm can provide extremely fast convergence with moderate accuracy, it requires some time to converge to the optimal filter coefficients. This is a well known characteristic of the LMS algorithm. Other adaption algorithms utilizing a gradient estimate will be investigated. Over short time scales, these will be slower to converge. However, over longer time scales, such gradient based algorithms may be quicker to arrive at the optimal coefficients. Furthermore, unlike the LMS algorithm, gradient based algorithms do not impose restrictions on the error signal. This may allow direct adaptive inverse control, such as that shown in Figure 2, without the additional complexity of FXLMS.

In this work, the goal was perfect plant inversion. No consideration was given to the magnitude of control signals required to do so. For systems that contain resonant zeros, a mechanism is required to limit the control signal magnitude. This may take the form of a penalty on control signal power or a limit on the maximum amplitude of any harmonic.

REFERENCES

[1] B. Potsaid, J. T. Wen, M. Unrath, D. Watt, and M. Alpay, "High performance motion tracking control for electronic manufacturing," *ASME Journal of Dynamic Systems, Measurement, and Control*, vol. 129, pp. 767–776, November 2007, mirror Scanner.

[2] E. Meyer, H. J. Hug, and R. Bennewitz, *Scanning probe microscopy. The lab on a tip*. Heidelberg, Germany: Springer-Verlag, 2004.

[3] S. M. Salapaka and M. V. Salapaka, "Scanning probe microscopy," *IEEE Control Systems Magazine*, vol. 28, no. 2, pp. 65–83, April 2008.

[4] D. Y. Abramovitch, S. B. Andersson, L. Y. Pao, and G. Schitter, "A tutorial on the mechanisms, dynamics, and control of atomic force microscopes," in *Proc. American Control Conference*, New York City, NY, July 2007, pp. 3488–3502.

[5] S. Devasia, E. Eleftheriou, and S. O. R. Moheimani, "A survey of control issues in nanopositioning," *IEEE Transactions on Control Systems Technology*, vol. 15, no. 5, pp. 802–823, September 2007.

[6] D. Y. Abramovitch, S. Hoen, and R. Workman, "Semi-automatic tuning of PID gains for atomic force microscopes," in *American Control Conference*, Seattle, WA, June 2008, pp. 2684–2689.

[7] S. S. Aphale, A. J. Fleming, and S. O. R. Moheimani, "A second-order controller for resonance damping and tracking control of nanopositioning systems," in *Proc. 19th International Conference on Adaptive Structures and Technologies*, Ascona, Switzerland, October 2008.

[8] A. J. Fleming, S. S. Aphale, and S. O. R. Moheimani, "A new robust damping and tracking controller for SPM positioning stages," in *Proc. American Control Conference*, St. Louis, MO, June 2009.

[9] T. Ando, N. Kodera, T. Uchihashi, A. Miyagi, R. Nakakita, H. Yamashita, and K. Matada, "High-speed atomic force microscopy for capturing dynamic behavior of protein molecules at work," *e-Journal of Surface Science and Nanotechnology*, vol. 3, pp. 384–392, December 2005.

[10] G. Schitter, K. J. Åström, B. E. DeMartini, P. J. Thurner, K. L. Turner, and P. K. Hansma, "Design and modeling of a high-speed AFM-scanner," *IEEE Transactions on Control Systems Technology*, vol. 15, no. 5, pp. 906–915, September 2007.

[11] A. D. L. Humphris, M. J. Miles, and J. K. Hobbs, "A mechanical microscope: high-speed atomic force microscopy," *Applied Physics Letters*, vol. 86, pp. 034 106–1–034 106–3, 2005.

[12] M. J. Rost, L. Crama, P. Schakel, E. van Tol, G. B. E. M. van Velzen-Williams, C. F. Overgauw, H. ter Horst, H. Dekker, B. Okhuijsen, M. Seynen, A. Vijftigschild, P. Han, A. J. Katan, K. Schoots, R. Schumm, W. van Loo, T. H. Oosterkamp, and J. W. M. Frenken, "Scanning probe microscopes go video rate and beyond," *Review of Scientific Instruments*, vol. 76, no. 5, pp. 053 710(1–9), April 2005.

[13] J. A. Butterworth, L. Y. Pao, and D. Y. Abramovitch, "A comparison of control architectures for atomic force microscopes," *Asian Journal of Control*, vol. Submitted, 2008.

[14] G. Schitter and A. Stemmer, "Identification and open-loop tracking control of a piezoelectric tube scanner for high-speed scanning-probe microscopy," *IEEE Transactions on Control Systems Technology*, vol. 12, no. 3, pp. 449–454, May 2004.

[15] S. Devasia, "Should model-based inverse inputs be used as feedforward under plant uncertainty?" *IEEE Transactions on Automatic Control*, vol. 47, no. 11, pp. 1865–1871, November 2002.

[16] Y. Wu and Q. Zou, "Iterative control approach to compensate for both the hysteresis and the dynamics effects of piezo actuators," *IEEE Transactions on Control Systems Technology*, vol. 15, no. 5, pp. 936–944, September 2007.

[17] K. Kim and Q. Zou, "Model-less inversion-based iterative control for output tracking: piezo actuator example," in *American Control Conference*, Seattle, WA, June 2008, pp. 2710–2715.

[18] Y. Li and J. Bechhoefer, "Feedforward control of a piezoelectric flexure stage for AFM," in *American Control Conference*, Seattle, WA, June 2008, pp. 2703–2709.

[19] A. J. Fleming, "Techniques and considerations for driving piezoelectric actuators at high-speed," in *Proc. SPIE Smart Materials and Structures*, San Diego, CA, March 2008.

[20] B. Widrow and E. Walach, *Adaptive inverse control*. Piscataway, NJ: IEEE Press, 2008, ebook.

[21] D. Croft, G. Shed, and S. Devasia, "Creep, hysteresis, and vibration compensation for piezoactuators: Atomic force microscopy application," *Transactions of the ASME, Journal of Dynamic Systems, Measurement, and Control*, vol. 123, pp. 35–43, March 2001.

[22] A. G. Hatch, R. C. Smith, T. De, and M. V. Salapaka, "Construction and experimental implementation of a model-based inverse filter to attenuate hysteresis in ferroelectric transducers," *IEEE Transactions on Control Systems Technology*, vol. 14, no. 6, pp. 1058–1069, November 2006.

[23] S. Bashash and N. Jalili, "A polynomial-based linear mapping strategy for feedforward compensation of hysteresis in piezoelectric actuators," *ASME Journal of Dynamic Systems, Measurement, and Control*, vol. 130, pp. 031 008(1–10), May 2008.

[24] J. G. Proakis and D. G. Manolakis, *Digital signal processing, 4th Ed.* New Jersey: Pearson Education Inc., 2007.

[25] B. Widrow and S. D. Stearns, *Adaptive signal processing*. Upper-Saddle River, NJ: Prentice Hall, 1985.

[26] A. J. Fleming and A. G. Wills, "Optimal periodic trajectories for band-limited systems," *IEEE Transactions on Control Systems Technology*, no. Accepted, 2008.
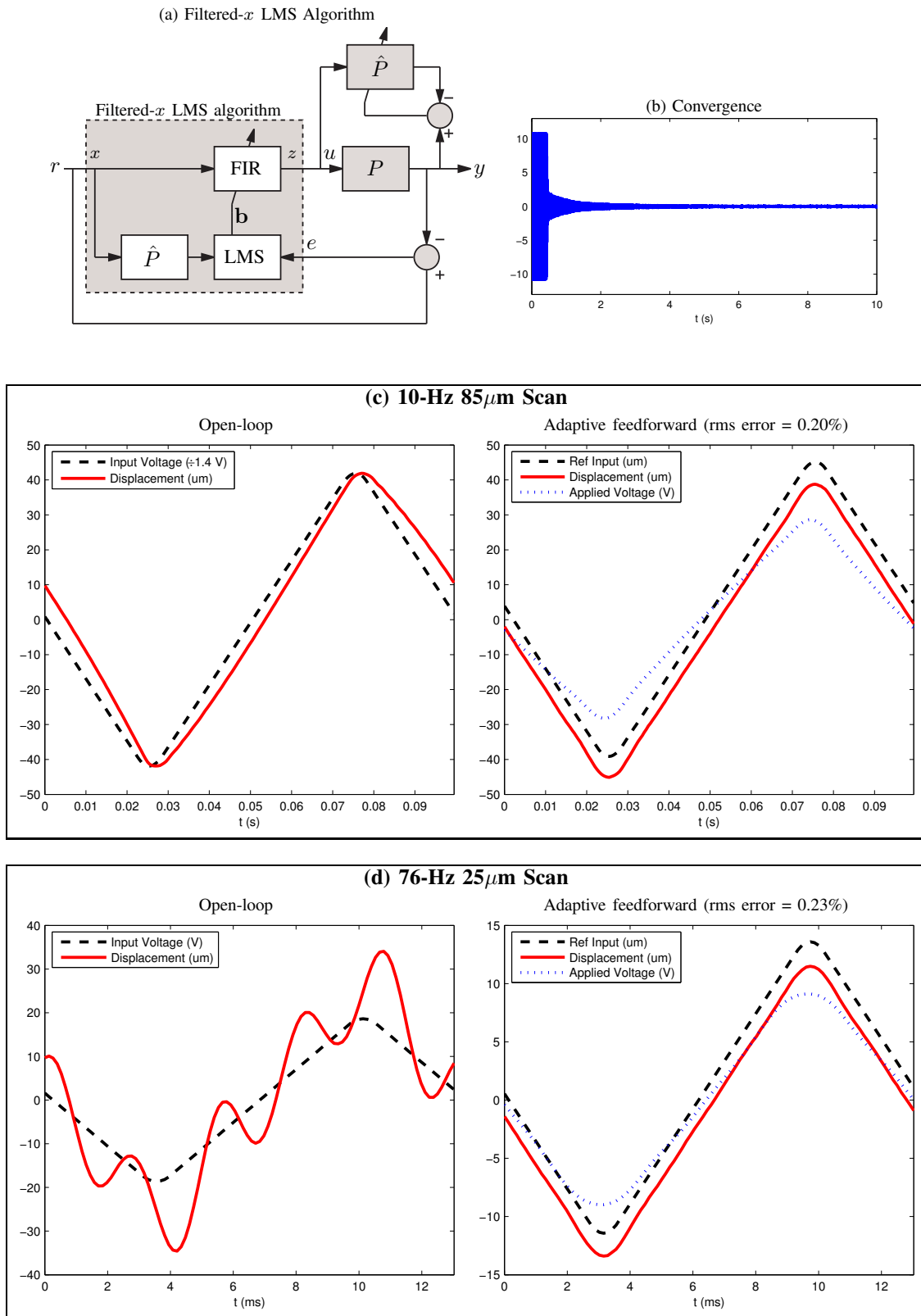
Fig. 6. The filtered-x LMS algorithm (a) employed for inverse feedforward control of the P-734 nanopositioning system. The response of the nanopositioner in open-loop and with feedforward control, to a 10-Hz and 76-Hz scan are plotted in subfigures (c) and (d). In these plots, the measured displacement is offset from the reference signal for the sake of clarity. The algorithm convergence characteristic during the 76 Hz scan is shown in Figure (b).